Theoretical Analysis of Non-ablative Laser Texturing of Silicon Surface with a Continuous Wave Fiber Laser

Hamid Farrokhi[*1], Wei Zhou[*1,2] and Hongyu Zheng[*3]

*[*1]School of Mechanical and Aerospace Engineering, Nanyang Technological University,50Nanyang Avenue, Singapore 639798*
E-mail: hami0006@e.ntu.edu.sg
*[*2]College of Materials Science and Engineering, Hefei University of Technology, Hefei 230009, P. R. China*
*[*3]Machining Technology Group, Singapore Institute of Manufacturing Technology, 71 Nanyang Drive, Singapore 638075*

Si is highly transparent to infrared fiber laser (λ=1090 nm) and the laser is not regarded as a suitable tool for ablation based silicon surface texturing. However, we have shown non-ablative texturing of Si surface is possible provided that suitable laser power and dwell time are chosen to produce peak surface temperature above the Si effective oxidation point of 1250 K and below the Si melting point of 1690 K. The phenomenon is explained through theoretical thermal analysis. The Kirchhoff transform is used to include the temperature dependent thermal conductivity. It is shown that with carefully adjusting laser parameters localized oxidation occurs and results in the formation of regularly patterned micro-bumps.

1. INTIRUCTION

Surface texturing became known as an important field of research with a broad range of applications in electronics, solar cells, and sensors. Focused ion beam (FIB), for instance, has been used to produce micro- and nano-scale surface patterns either by direct FIB writing [1-3] or through ion beam induced self-organization [4-6]. However, this type of patterning has to be conducted in high vacuum for very small surface areas. In contrast, laser beam can be used to pattern surface in ambient or controlled environments over large surface areas [7-9].

Si is an important semiconductor material, so texturing its surface by laser has been well studied in the past [10-14]. However, all the surface texturing is based upon *ablation*. Hardly any report can be found on use of non-ablative laser surface texturing to form uniform micro-patterns. Recently, we succussed to pattern Si surface by *non-ablative* laser texturing using continuous wave fiber laser (λ=1090 nm) [15-17]. As Si is known to be highly transparent to the infrared wavelength, the fiber laser is not regarded as a suitable tool for texturing of Si surface. We elucidated the non-ablative surface texturing in terms of laser-induced localized thermal oxidation [15, 16]. However, the current study aimed to gain better understanding of the non-ablative texturing mechanism through theoretical thermal analysis and to provide a quick-estimation tool for determining the suitable laser parameters for the surface texturing. The non-ablative texturing method provides possibilities for micro/nano-device applications, clean and free-crack marking of silicon wafers.

2. EXPERIMENATL PROCEDURE AND RESULTS

The material used in the study was a single crystal (100) n-type (phosphorous doped) Si wafer with resistivity ρ = 1-20 Ω·cm and thickness of 300 μm. The wafer was cut into smaller pieces in the size of 10 mm × 10 mm. Ultrasonic cleaning of the samples was carried out in methanol for 10 min, acetone for another 10 min, and then de-ionized water for 30 min. To minimize influence of native oxide layer, the cleaned samples were kept in de-ionized water till being used.

The samples were mounted on a motorized X-Y precision stage and irradiated using a continuous wave fibre laser with wavelength λ = 1090 nm. The laser scanning was carried out in an area of 2 mm × 2 mm with a point scanning pitch of 20 μm, as shown in Figure 1. A lens of 50 mm focal length was used to focus the laser beam to the size of ≈ 20 μm.

The laser experiments were carried out using varying laser power (11.5, 19, or 23.3 W) and dwell time (10, 20, 30, or 40 ms) in O_2 atmosphere. O_2 was delivered onto the Si surface in the pressure of 0.5 bar through a coaxial nozzle with an exit diameter of 2 mm and placed about 2 mm above the surface, as shown in Figure 1.

Surfaces irradiated with the fiber laser were carefully observed under the confocal microscope and the 3D optical profilometer. We summarize our observation as follows:

(1) No discernible change was found on surface irradiated using the lowest power of 11.5 W.
(2) Considerable morphological changes were found on surface irradiated with the highest power of 23.3 W, but the surface patterns were irregular, as shown in Figure 2(a).
(3) When the moderate power of 19 W was used, regularly patterned surface features were formed when the dwell time was 40 ms, as shown in Figure 2(b); however, no such uniform surface patterns were observed for the

lower dwell times (10, 20, or 30 ms). The regularly patterned surface was further studied using 3D optical profilometer, as shown in Figures 3(a) and 3(b).
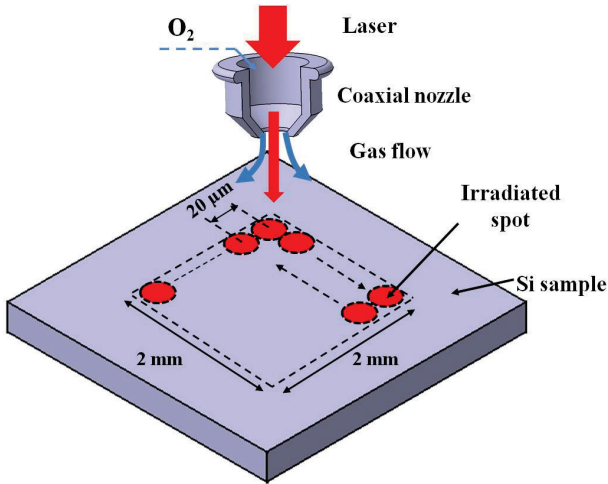

Fig. 1 Illustration of experimental setup

Fig. 2 Confocal microscope images of surface irradiated with (a) laser power of 23.3 W, dwell time of 40 ms and (b) laser power of 19 W, dwell time of 40 ms.

Figure 3(a) shows 3D image of the uniformly patterned surface irradiated with laser power=19W and dwell time=40ms. Figure 3(b) demonstrates 2D profile of a bump with height of ≈750nm and base diameter of about 13µm. More detailed description of the experimental data could be found in [15].

In the following sections, we will attempt to elucidate the phenomena by theoretical thermal analysis.

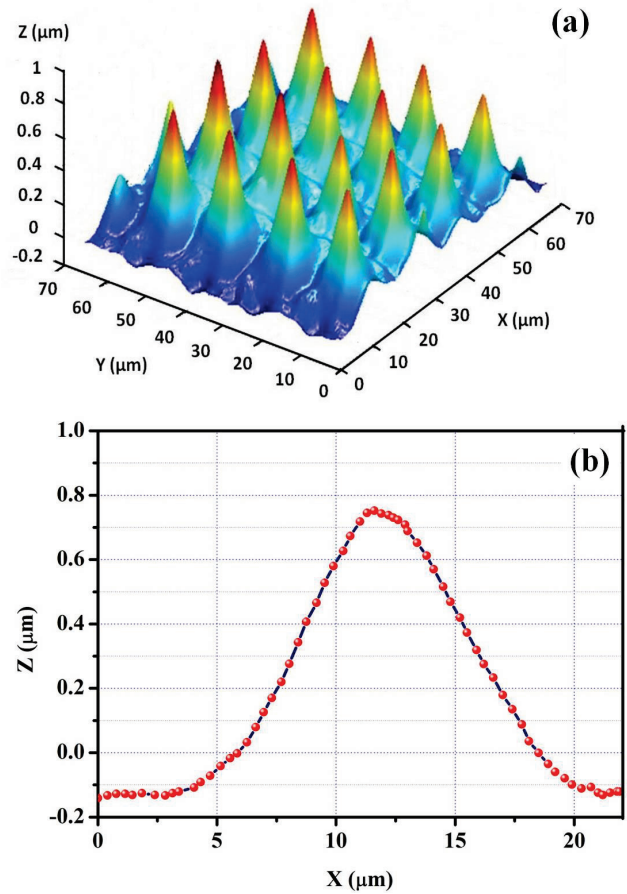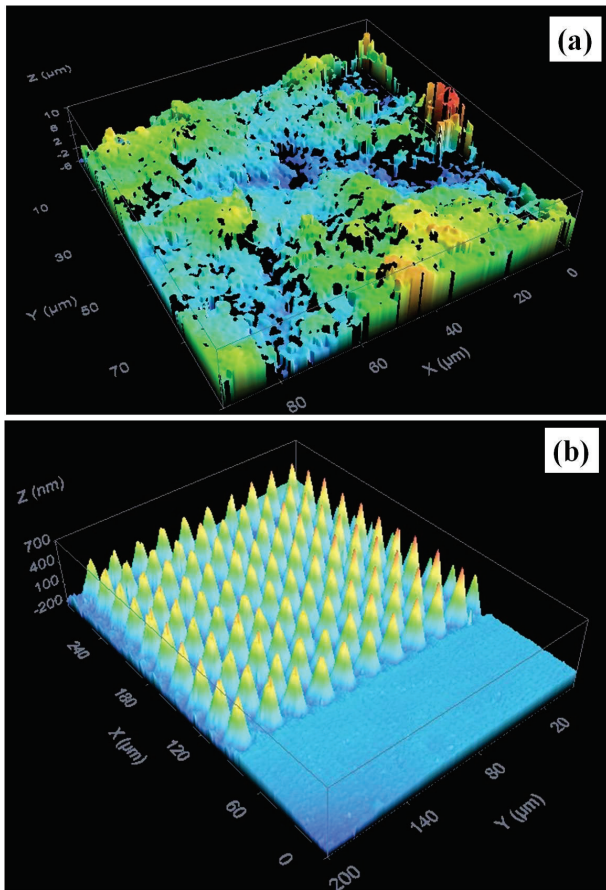**Fig. 3** (a) 3D optical image of surface irradiated with laser power: 19 W and dwell time: 40 ms. (b) 2D profile of a bump shown in (a).

3. Theoretical Analysis
3.1. Kirchhoff transform - linear and true temperature

The familiar heat transfer equation for the temperature, T, is the diffusion equation:

$$\rho C_p(T)\frac{\partial T}{\partial t} = \nabla\left[k(T)\nabla T\right] + Q(r,t) \tag{1}$$

where k is the thermal conductivity, ρ the density, and C_p the specific heat of the material, and $Q(r,t)$ is rate at which energy is being supplied to the material. The density and specific heat can be assumed to be constant for Si, but the thermal conductivity varies approximately as $1/T$ above room temperature. Thus equation (1) is strongly nonlinear.

The nonlinear heat flow equation can be simplified by introducing the Kirchhoff transformation [18]:

$$\theta(t) = \int_{T_0}^{T(t)}\frac{k(T')}{k_0}dT' \tag{2}$$

where k_0 is the thermal conductivity at a reference temperature T_0, which is chosen to be the initial substrate temperature.

The linear temperature rise, $\theta(t)$, is then related to the true temperature rise, T(t), by equation (2). In the steady-state condition, the equation for θ is the linear heat flow equation, and therefore we name θ the linear temperature. The temperature distribution for the steady-state can thus be obtained by first solving the linear heat flow equation for θ, with constant conductivity k_0. The true temperature T is then calculated by using the inverse of Kirchhoff transform [19, 20].

The thermal conductivity of Si can be adequately approximated using equation (3)[20].

$$k_T = A / (T - B) \tag{3}$$

where A = 299 W/cm and B = 99 K. Thus, the inverse of Kirchhoff transform can be expressed analytically as below:

$$T = B + (T_0 - B)\exp[\theta(t) / (T_0 - B)] \tag{4}$$

Spatial intensity distribution of the laser is considered to be :

$$I = (P_{abs} / \pi w^2)\exp(-r^2 / w^2) \tag{5}$$

where r is the distance from the center of the beam and P_{abs} is the total absorbed power. w is beam radius at the 1/e of the peak power.

The beam is centered on the point of interest, (x,y)=(0,0), at time t=0. The maximum linear temperature rise at t=0 is derived as below.

$$\theta_{max} = \frac{P_{abs}}{2\sqrt{\pi} w k_0} \tag{6}$$

The results of equation (6) can now be inserted into equation (4) to calculate the maximum true temperature rise.

$$T_{max} = B + (T_0 - B)\exp\left[\frac{P_{abs}}{2\sqrt{\pi} wA}\right] \tag{7}$$

Noted that the equation (7) is derived to calculate the maximum surface temperature rise in the steady-state condition. Thus, in the next section we have specified the condition.

3.2. Temperature versus time for constant intensity

The condition in which the steady-state solution for solving the heat equation can be used is determined using numerical method.

Because of the nonlinearity of equation (1), we have chosen the three time level implicit method for numerical solution of the temperature. The thermal conductivity is given by equation (3). We use ρ=2.3 g/cm³ and C_p=0.88 J/gK for the density and specific heat of Si. For simplicity we assume a single absorption coefficient, α=50 1/cm. The value of the absorption coefficient has little effect on how quickly the equilibrium is achieved.

Figure 4 shows the results of numerical method for a 300 μm thick sample subjected to incident power of 23.3, 19, and 11.5 W with T_0=298 K. It is shown that 98% of the final temperature rise is reached within 10ms, and after 15 ms the sample is in relative steady-state. This means that the steady-state solution for the temperature can be reasonably used if half of the irradiation dwell time is more than 15 ms. It implies that the steady-state solution could be valid for the dwell time above 30ms.

Since the condition for the steady-state will normally be met in experiments with CW fiber laser and dwell time of 40ms, we will limit the study to the time-independent case..
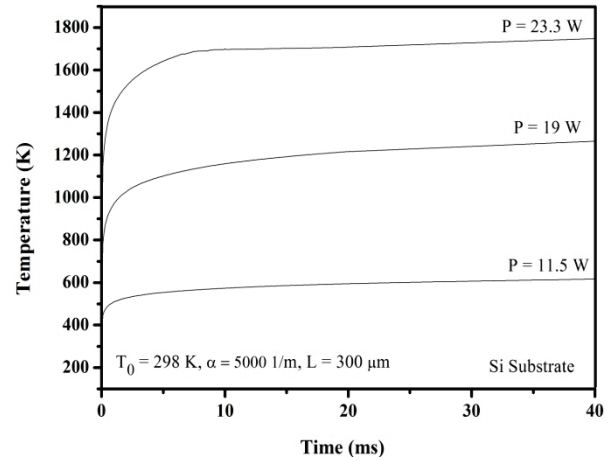
Fig. 4 Surface temperature vs time of a Si sample irradiated with a constant incident power of 23.3, 19, 11.5 W. The absorption coefficient α is 5000 1/m; and sample thickness is 300 μm. The results are obtained numerically.

3.3. Temperature rise in the steady-state condition

We have demonstrated that the steady-state solution is applicable for CW irradiation with the dwell time above 30ms. Equation (7) is used to obtain the maximum surface temperature for various incident powers (11.5, 19, 23.3 W) at fixed dwell time of 40ms. The results are shown in Table1.

Table1 Maximum surface temperature at various incident laser power.

Incident laser power (W)	11.5	19	23.3
T_{max} (K) (steady-state)	688	1294	1892
T_{max} (K) (Numerical)	610	1265	1760
T_{max} (K) (FE) [16]	619	1304	1840
Dwell time = 40 ms, R = 0.33, T=0.51			

To obtain the absorbed power , P_{abs} , the following equation has been used.

$$P_{abs} = (1 - R - T)P_{inc} \tag{8}$$

where P_{inc} is incident laser power, R and T are reflection and transmission coefficient of Si at the fiber laser wavelength (1090nm).

It is shown that for dwell times above 30 ms, the surface temperature rise obtained through steady-state solution is in fair agreement with that of obtained through numerical method and finite element (FE) analysis [16] . It suggests that the steady-state solution could be quick-estimation tool for determining the suitable laser parameters for non-ablative surface texturing comparing with time-consuming numerical method.

4. Discussion

Results of the maximum surface temperature at center of the irradiated point are shown in Table 1. For the highest laser power of 20.3 W, It shows that the surface temperature is above the melting point of Si (1690 K). . This explain the formation of irregular surface patterns when the surface is irradiated with this laser power (see Figure 2(a)). The result is in good agreement with that of obtained through FE study [16].

It can be found from Table 1 that no melting would occur on surfaces irradiated with laser power of 11.5 W and 19 W for dwell time = 40 ms, since the surface temperature is below the melting point of Si. It shows good agreement with our previous study carried out using FE analysis [16].

If localized thermal oxidation of Si accounts for formation of the regular bumps as suggested earlier [15], regular bumps might be expected to form for laser power of both 11.5 W and 19 W. However, in reality, regular surface bumps were formed only when the laser power was 19 W and the dwell time was 40 ms. The thermal analysis results may help to explain why this is the case.

It is found in many studies [21-25] that thermal oxidation of Si surface generally occurs in the temperature range 1000–1600 K and that 56% of the oxide thickness rises above the original silicon surface. For the laser power of 11.5 W, the steady-state solution, numerical method and FE study [16] showed the peak temperature is well below 1000 K (see Table 1). Therefore, it is understandable why no surface bumps were formed due to thermal oxidation for this laser power.

For laser power of 19 W, numerical method (see Fig.4) and FE study [16] showed the peak temperature is above 1000 K for all the dwell times used (10, 20, 30, and 40 ms). In addition, steady-state solution which is valid for dwell time above 30 ms shows the same finding for the dwell time of 40ms. However, it is noticed that regular bumps formed only when the longest dwell time (40 ms) was used. This interesting phenomenon is believed to be related to decrease of activation energy of Si oxidation with increasing temperature.

Activation energy of Si oxidation lies around 2-2.5 eV for temperature range 1100 to 1200 K, but the value decreases to 1.3 eV when the temperature reaches 1250 K [23]. In the current study, an infrared laser with wavelength 1090 nm was used. Photon energy for this laser is calculated as E_{photon} =1.138 eV. When the temperature is below 1250 K, the photon energy is well below the activation energy of Si oxidation (which is 2-2.5 eV for temperature range 1100-1200 K and 1.3-2 eV for temperature range 1200-1250 K [23]), making it difficult for effective Si oxidation to occur at temperatures below 1250 K. When the laser power is 19 W and dwell time is 10 ms or 20 ms, numerical method and FE study [16] showed the peak temperature is below 1250 K, so no effective Si oxidation occurs.

When the temperature rises to 1250 K, the activation energy of Si oxidation is reduced to 1.3 eV, which is very close to but still above the value of photon energy (1.138 eV). When the temperature rises further, the activation energy reduces further. Therefore, at a certain temperature above 1250 K, the activation energy falls below the photon energy, making it possible for the effective oxidation of Si to occur and resulting in localized surface expansion and bump formation.

For laser power of 19 W and dwell time of 30 ms numerical method and FE study [16] showed that the peak temperature is just above 1250 K. The fact that no bumps were observed on the laser irradiated surface suggests that the activation energy at this peak temperature is not yet reduced to below the photon energy level.

When the dwell time is increased to 40 ms, steady-state solution as well as numerical method and FE study [16] shows the peak temperature increases well above effective oxidation temperature (1250 K). It is shown to be 1294 K obtained by steady-state solution (see Table 1). The fact that bumps were observed on the laser irradiated surface indicates that the activation energy at 1294 K is reduced to below the photon energy. It can be deduced from the analyses that the critical temperature for effective oxidation of Si is somewhere between 1250 and 1300 K. The temperature of 1250 K is used as the lower boundary for effective oxidation, and the upper boundary is naturally the melting point (1690 K).

Furthermore, steady-state solution might be quick-estimation tool to predict a range of laser powers suitable for making oxide bumps through the non-ablative method. Figure 5 shows various incident laser powers at dwell time of 40ms which can be used for the purpose of surface texturing.
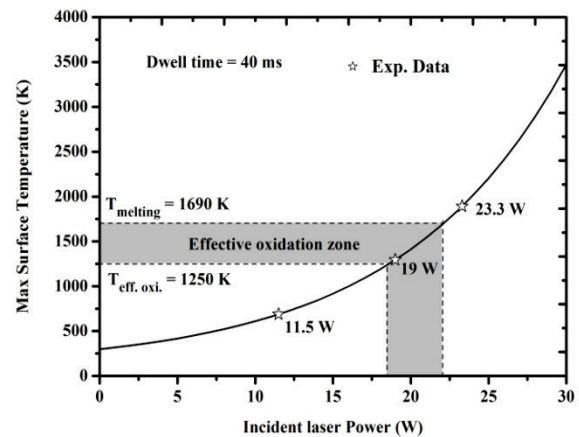

Fig. 5 Maximum surface temperature vs incident laser power obtained through steady-state thermal analysis, showing the effective oxidation zone to produce regular bumps on Si surface.

Estimated power range gives the maximum surface temperature which falls between the two temperature boundary lines named as effective oxidation zone.

5. Conclusions

A regular array of micro-bumps was fabricated on Si surface using continuous wave fiber laser (λ = 1090 nm) based on laser induced non-ablative texturing. Steady-state thermal analysis was used to explain the formation phenomenon. The condition for using the steady-state solution was obtained by numerical method. It is found that the bumps formation is due to laser-induced localized Si oxidation. A range of laser powers at the fixed dwell time of 40ms, suitable for the non-ablative surface texturing, was determined using theoretical results and it is named as the effective oxidation zone. The solution might be used as a quick-estimation tool to specify the suitable laser power to produce uniformly patterned surface features on Si.

References

[1] H. X. Qian, Z. Wei, M. Jianmin, E. N. L. Lennie, and X. R. Zeng: *J. Micromech. Microeng.*, 18, (2008) 035003.
[2] Y. Fu, N. Bryan, and W. Zhou: Opt. Express, 12, (2004) 1803.
[3] Y. Fu, W. Zhou, L. E. N. Lim, C. Du, X. Luo, Z. Zhao, X. Dong, H. Shi, and C. Wang: Opt Eng, 45, (2006) 108001.
[4] J. Lian, W. Zhou, Q. M. Wei, L. M. Wang, L. A. Boatner, and R. C. Ewing: Appl. Phys. Lett., 88, (2006) 093112.
[5] H. X. Qian, W. Zhou, Y. Q. Fu, B. K. A. Ngoi, and G. C. Lim: Appl. Surf. Sci., 240, (2005) 140.
[6] H. X. Qian, and W. Zhou: Mater. Lett. , 77, (2012) 113.
[7] H. Y. Zheng, W. Zhou, H. X. Qian, T. T. Tan, and G. C. Lim: Appl. Surf. Sci. , 236, (2004) 114.
[8] H. X. Qian, W. Zhou, H. Y. Zheng, and G. C. Lim: Surf. Sci., 595, (2005) 49.
[9] Z. L. Li, T. Liu, C. C. Khin, A. C. Tan, L. E. Khoong, H. Y. Zheng, and W. Zhou: Opt. Express, 18, (2010) 15990.
[10] T.-H. Her, R. J. Finlay, C. Wu, S. Deliwala, and E. Mazur: Appl. Phys. Lett., 73, (1998) 1673.
[11] V. Zorba, I. Alexandrou, I. Zergioti, A. Manousaki, C. Ducati, A. Neumeister, C. Fotakis, and G. A. J. Amaratunga: Thin Solid Films, 453–454, (2004) 492.
[12] V. Zorba, P. Tzanetakis, C. Fotakis, E. Spanakis, E. Stratakis, D. G. Papazoglou, and I. Zergioti: Appl. Phys. Lett., 88, (2006) 081103.
[13] P. Simon, and J. Ihlemann: Appl. Surf. Sci., 109-110, (1997) 25.
[14] B. Borchers, J. Bekesi, P. Simon, and J. Ihlemann: J. Appl. Phys., 107, (2010) 063106.
[15] H. Farrokhi, W. Zhou, H. Y. Zheng, and Z. L. Li: Opt. Express, 20, (2012) 23180.
[16] H. Farrokhi, w. Zhou, H. Zheng, and Z. Li: J. Comput. Theor. Nanosci., 11, (2014) 1.
[17] H. Farrokhi, W. Zhou, H. Y. Zheng, and Z. Li: Proc. of SPIE Vol. 7926, p. 792607.
[18] H. S. Carslaw, and J. C. Jeager: "Conduction of Heat in Solids", (Clarendon Press, Oxford 1986).
[19] M. Lax: J. Appl. Phys., 48, (1977) 3919.
[20] Y. I. Nissim, A. Lietoila, R. B. Gold, and J. F. Gibbons: J. Appl. Phys., 51, (1980) 274.
[21] J. Blanc: Appl. Phys. Lett., 33, (1978) 424.
[22] V. K. Samalam: Appl. Phys. Lett., 47, (1985) 736.
[23] A. Fargeix, and G. Ghibaudo: J. Appl. Phys., 56, (1984) 589.
[24] H. Z. Massoud, J. D. Plummer, and J. D. Irene: J. Electrochem. Soc, 132, (1985) 2693.
[25] B. E. Deal, and A. S. Grove: J. Appl. Phys., 36, (1965) 3770.